Mon. Not. R. Astron. Soc. **348,** 123–138 (2004)

Smoothed Particle Magnetohydrodynamics – I. Algorithm and tests in one dimension

D. J. Price[1]★ and J. J. Monaghan[2]

[1]*Institute of Astronomy, Madingley Road, Cambridge CB3 0HA*
[2]*School of Mathematical Sciences, Monash University, Clayton 3800, Australia*

Accepted 2003 October 22. Received 2003 October 21; in original form 2003 June 6

ABSTRACT

In this paper we show how the Smoothed Particle Hydrodynamics (SPH) equations for ideal Magnetohydrodynamics (MHD) can be written in conservation form with the positivity of the dissipation guaranteed. We call the resulting algorithm Smoothed Particle Magnetohydrodynamics (SPMHD). The equations appear to be accurate, robust and easy to apply and do not suffer from the instabilities known to exist previously in formulations of the SPMHD equations. In addition we formulate our MHD equations such that errors associated with non-zero divergence of the magnetic field are naturally propagated by the flow and should therefore remain small.

In this and the companion paper we present a wide range of numerical tests in one dimension to show that the algorithm gives very good results for one-dimensional flows in both adiabatic and isothermal MHD. For the one-dimensional tests the field structure is either two- or three-dimensional.

The algorithm has many astrophysical applications and is particularly suited to star-formation problems.

Key words: magnetic fields – MHD – methods: numerical.

1 INTRODUCTION

Star-forming regions are known to contain magnetic fields which are sufficiently strong to play an important part in the formation of the dense concentrations of matter which lead to stars. In order to describe the dynamics of such a system it is customary to begin with the equations of ideal Magnetohydrodynamics (MHD). However, the simplicity of the MHD equations is deceptive and hides the fact that there are numerous technical difficulties involved in their solution. Our aim in this paper is to describe a set of Smoothed Particle Hydrodynamics (SPH, for a review see Monaghan 1992) equations which overcome these difficulties and can be used to simulate MHD phenomena. We call the resulting algorithm Smoothed Particle Magnetohydrodynamics (SPMHD). The equations appear to be accurate, robust and easy to apply and they do not suffer from the instabilities that exist in other formulations of the SPMHD equations.

An early application of SPH to MHD problems was to static magnetic polytropes by Gingold & Monaghan (1977) who found good agreement with perturbation calculations. Dynamical problems were considered by Phillips (1983b) and applied to star-formation problems (Phillips 1982, 1983a, 1985, 1986a,b; Benz 1984; Phillips & Monaghan 1985). In the latter it was shown that when the conservation form of the equations was used an instability developed which took the form of clumping of SPH particles. SPH blast waves in a magnetic medium were studied by Stellingwerf & Peterkin (1990, 1994). Habe et al. (1991), Murray, Wadsley & Bond (1996) and Mac Low et al. (1999) used a form of the SPH equations where the magnetic fields were updated on a grid and interpolated to the SPH particles.

Meglicki (1994, 1995) and Meglicki, Wickramasinghe & Dewar (1995) used a formulation of SPMHD that uses a non-conservative ($\boldsymbol{J} \times \boldsymbol{B}$) force, which is always stable and guarantees that the magnetic force is exactly perpendicular to the magnetic field. This formalism was also used by Byleveld & Pongracic (1996) and more recently by Cerqueira & de Gouveia Dal Pino (2001, and references therein) and Hosking (2002); however, the non-conservation of momentum leads to poor performance on shock-type problems. A conservative form of SPMHD has been used by Dolag, Bartelmann & Lesch (1999) and by Marinho, Andreazza & Lépine (2001) since the magnetic field in their simulations remained in the regime where the instability does not appear. Morris (1996) suggested using a compromise between the conservative (tensor) force and the $\boldsymbol{J} \times \boldsymbol{B}$ formalism. Non-ideal MHD terms in SPH were also considered by Morris (1996), who suggested using resistive terms to control the divergence of the magnetic field, and by Hosking (2002), who considered the effects of ambipolar diffusion via a two-fluid model.

The first technical difficulty with MHD simulations is that the magnetic field comes with the constraint that $\nabla \cdot \boldsymbol{B} = 0$.

★E-mail: dprice@ast.cam.ac.uk

Brackbill & Barnes (1980) showed that in some finite difference codes, the failure to satisfy this constraint would lead to an instability. A number of different techniques have therefore been developed to ensure that this constraint is satisfied. The first of these is to work with the vector potential $\boldsymbol{A}$ where $\boldsymbol{B} = \nabla \times \boldsymbol{A}$ rather than with $\boldsymbol{B}$. This approach was used by Gingold & Monaghan (1977) for SPH simulations. Others (Evans & Hawley 1988; Stone & Norman 1992) construct their finite difference equations so that, to the accuracy of the resolution, $\nabla \cdot \boldsymbol{B} = 0$. Another approach commonly used is to clean up the magnetic field at every step by adding a gradient term to the computed field to produce a new field which satisfies the constraint. By giving up the conservation of momentum and including $\nabla \cdot \boldsymbol{B}$ terms in the momentum equation Powell (1994) (see Powell et al. 1999) produced a stable finite difference scheme for MHD (the eight-wave theory) which, however, appears to be less accurate for shocks. A comprehensive discussion of these and other schemes has been given by Tóth (2000) who notes that even if $\nabla \cdot \boldsymbol{B} = 0$ most of these schemes produce magnetic forces which are not perpendicular to the exact magnetic force $\boldsymbol{J} \times \boldsymbol{B}$. Within the framework of SPH, Børve (2001) (see Børve, Omang & Trulsen 2001) developed a non-conservative form of the SPMHD equations which have good stability properties and by the creation of closely spaced particles in regions with large spatial gradients it gives excellent accuracy.

An alternative to any of these approaches is that of Janhunen (2000) who starts from the premise that non-zero $\nabla \cdot \boldsymbol{B}$ terms may be generated but, if they are treated consistently, no instabilities will occur. The resulting set of equations has been derived by Dellar (2001) starting with the relativistic formulation of gas dynamics with electromagnetic fields. Janhunen (2000) showed that this formulation of MHD gas dynamics could be simulated using the HLL method (Harten et al. 1983) and he showed by thousands of test cases that positivity could be expected even if not proven.

Our approach is to follow Janhunen (2000) and use equations that are consistent even if $\nabla \cdot \boldsymbol{B}$ does not vanish. To simulate shocks we introduce an artificial dissipation which guarantees that changes to entropy and thermal energy from viscous and ohmic dissipation are positive. The resulting set of equations conserves momentum and energy exactly.

Another technical difficulty peculiar to SPH is that when a conservative force is used the SPH particles tend to clump in pairs in the presence of tension. This was first noticed by Phillips & Monaghan (1985) and re-discovered by researchers applying SPH to elastic fracture problems (see the references in Monaghan 2000). Several remedies have been proposed (e.g. Dyka, Randles & Ingel 1997; Bonet & Kulasegaram 2000, 2001) but they all either involve a significant increase in computation or cannot be applied where the particle configuration changes significantly. A remedy for the tensile instability which can be easily applied to astrophysical problems was proposed by Monaghan (2000). The idea is to add a small artificial stress which prevents particles from clumping in the presence of a negative stress. This term has been shown to work well in elastic dynamics simulations (Gray, Monaghan & Swift 2002) and we apply it here to the MHD case. We find that such a term very effectively removes the instability with few side-effects.

In Section 2 we give the continuum form of the equations, and in Section 3 the SPH form of these equations. We construct appropriate dissipation terms for MHD in Section 4. The instability correction is discussed in Section 5 with details in Appendix A. The time-stepping strategy is described in Section 6. In Section 7 we present the results of extensive numerical tests for one-dimensional problems involving discontinuous initial conditions. In the companion paper (Price & Monaghan 2003, hereafter Paper II) we derive the SPMHD equations from a variational principle, including the case where the smoothing length is regarded as a function of local particle density. A self-consistent derivation of the SPMHD equations in the latter case is shown to increase the accuracy of SPMHD wave propagation. Two- and three-dimensional tests will be presented elsewhere.

2 THE CONTINUUM EQUATIONS

In the absence of dissipation the ith component of the acceleration equation is

$$\frac{\mathrm{d}v^i}{\mathrm{d}t} = \frac{1}{\rho}\frac{\partial S^{ij}}{\partial x^j}, \tag{1}$$

where $\mathrm{d}/\mathrm{d}t$ denotes the derivative following the motion, and the stress S^{ij} in the case of ideal MHD is defined by

$$S^{ij} = -P\delta^{ij} + \frac{1}{\mu_0}\left(B^i B^j - \frac{1}{2}\delta^{ij}B^2\right). \tag{2}$$

Here B^i is the ith component of the magnetic field and μ_0 is the permittivity of free space. For SI units $\mu_0 = 4\pi/10^7$.

The time change of the magnetic field is given by the induction equation. We follow Janhunen (2000) and Dellar (2001) and construct the induction equation so that it is consistent even if $\nabla \cdot \boldsymbol{B}$ does not vanish. The induction equation including ohmic dissipation then becomes

$$\frac{\partial \boldsymbol{B}}{\partial t} + \nabla \times (\boldsymbol{v} \times \boldsymbol{B}) = -\nabla \times (\eta \boldsymbol{J}) - \boldsymbol{v}(\nabla \cdot B), \tag{3}$$

where the last term is the magnetic current (Janhunen 2000; Dellar 2001) and $\boldsymbol{J}$ is the normal current

$$\boldsymbol{J} = \mu_0 \nabla \times \boldsymbol{B}, \tag{4}$$

and η is the magnetic diffusivity $1/(\sigma\mu_0)$ where σ is the conductivity.

This induction equation can be written

$$\frac{\mathrm{d}\boldsymbol{B}}{\mathrm{d}t} = (\boldsymbol{B} \cdot \nabla)\boldsymbol{v} - \boldsymbol{B}(\nabla \cdot \boldsymbol{v}) - \nabla \times (\eta \boldsymbol{J}). \tag{5}$$

This last form of the induction equation is the standard form when the constraint $\nabla \cdot \boldsymbol{B} = 0$ is used. Magnetic monopoles associated with $\nabla \cdot \boldsymbol{B} \neq 0$ do not affect this equation. Taking the divergence of (3), we find that monopoles evolve according to

$$\frac{\partial}{\partial t}(\nabla \cdot \boldsymbol{B}) + \nabla \cdot (\boldsymbol{v}\nabla \cdot \boldsymbol{B}) = 0, \tag{6}$$

which has the same form as the continuity equation for the density and therefore implies that the volume integral of $\nabla \cdot \boldsymbol{B}$ is conserved.

It is common to solve the acceleration equation with the thermal energy and continuity equations, but in this section we will assume that the thermal energy equation is replaced by the total energy equation. Our aim is to derive a set of SPH equations which conserve total energy and momentum while ensuring that the change in entropy due to dissipation is positive.

The total energy e per unit volume is defined by

$$e = \rho\left(\frac{1}{2}v^2 + u + \frac{B^2}{\rho\mu_0}\right), \tag{7}$$

where u is the thermal energy per unit mass. The equation for the rate of change of e can be written in terms of the stress according to

$$\frac{\partial e}{\partial t} = -\nabla \cdot (e\boldsymbol{v}) + \frac{\partial (v^i S^{ij})}{\partial x^j} + \nabla \cdot [\boldsymbol{B} \times (\eta \boldsymbol{J})], \tag{8}$$

or as

$$\frac{\partial e}{\partial t} = -\nabla \cdot \left[\left(e + P + \frac{B^2}{2\mu_0} \right) \boldsymbol{v} - \frac{\boldsymbol{B}(\boldsymbol{v} \cdot \boldsymbol{B})}{\mu_0} - \boldsymbol{B} \times (\eta \boldsymbol{J}) \right]. \quad (9)$$

To derive SPH equations it is convenient to replace the energy per unit volume by the energy per unit mass $\widehat{\epsilon}$:

$$\widehat{\epsilon} = \frac{1}{2} v^2 + u + \frac{B^2}{2\rho\mu_0}. \quad (10)$$

The equation for $\widehat{\epsilon}$ is

$$\frac{\mathrm{d}\widehat{\epsilon}}{\mathrm{d}t} = \frac{1}{\rho} \frac{\partial (S^{ij} v^j)}{\partial x^j} + \frac{1}{\rho} \nabla \cdot [\boldsymbol{B} \times (\eta \boldsymbol{J})]. \quad (11)$$

The thermal energy equation can be derived either from (10) giving

$$\frac{\mathrm{d}u}{\mathrm{d}t} = \frac{\mathrm{d}\widehat{\epsilon}}{\mathrm{d}t} - \boldsymbol{v} \cdot \frac{\mathrm{d}\boldsymbol{v}}{\mathrm{d}t} - \frac{\mathrm{d}}{\mathrm{d}t} \left(\frac{B^2}{2\mu_0 \rho} \right), \quad (12)$$

or by using the first law of thermodynamics including the ohmic heating term. Either way we find

$$\frac{\mathrm{d}u}{\mathrm{d}t} = -\frac{P}{\rho} \nabla \cdot \boldsymbol{v} + \eta J^2, \quad (13)$$

The final equation is the density equation

$$\frac{\mathrm{d}\rho}{\mathrm{d}t} = -\rho \nabla \cdot \boldsymbol{v}. \quad (14)$$

In addition we need an equation of state and an expression for the conductivity. In this paper we assume the gas is an ideal gas and we introduce an artificial dissipation into the SPH equations which we then interpret in terms of an artificial viscosity, thermal conductivity and magnetic diffusivity.

3 THE SPH EQUATIONS

We take as our fundamental equations the acceleration equation, the total energy equation and the density equation. To construct our SPMHD equations we follow the procedure used for the special relativistic equations (Chow & Monaghan 1997). Initially the equations will be set up assuming there is no ohmic dissipation. We will introduce artificial dissipation in the SPMHD equations in order to handle shocks and we will then show that to guarantee that the ohmic dissipation is always positive we must include an extra term in the induction equation. This extra term gives the appropriate extension of the induction equation to include the effects of an artificial conductivity.

The acceleration equation for SPH particle a is (Monaghan 1992)

$$\frac{\mathrm{d}v_a^i}{\mathrm{d}t} = \sum_b m_b \left(\frac{S_a^{ij}}{\rho_a^2} + \frac{S_b^{ij}}{\rho_b^2} + \Pi_{ab} \right) \frac{\partial W_{ab}}{\partial x_a^j}, \quad (15)$$

where $W_{ab} = W(|\boldsymbol{r}_a - \boldsymbol{r}_b|, h)$ is the smoothing kernel. The dissipation term Π_{ab} will be discussed shortly. We write the energy equation in the absence of ohmic dissipation in the form

$$\frac{\mathrm{d}\widehat{\epsilon}}{\mathrm{d}t} = v^i \frac{\partial}{\partial x^j} \left(\frac{S^{ij}}{\rho} \right) + \frac{S^{ij}}{\rho^2} \frac{\partial (\rho v^i)}{\partial x^j}, \quad (16)$$

which is similar to that used for special relativistic SPH (Chow & Monaghan 1997). The SPH equivalent of this equation is

$$\frac{\mathrm{d}\widehat{\epsilon}_a}{\mathrm{d}t} = \sum_b m_b \left(\frac{v_a^i S_b^{ij}}{\rho_b^2} + \frac{v_b^i S_a^{ij}}{\rho_a^2} + \Omega_{ab} \right) \frac{\partial W_{ab}}{\partial x_a^j}, \quad (17)$$

where Ω_{ab} is a dissipation term analogous to Π_{ab}. Because of the symmetry of the terms in the summation, total linear momentum $\sum_a m_a \boldsymbol{v}_a$, and energy $\sum_a m_a \widehat{\epsilon}_a$ are conserved.

The induction equation in the absence of the ohmic term can be written as

$$\frac{\mathrm{d}B^i}{\mathrm{d}t} = \frac{B^j}{\rho} \frac{\partial}{\partial x^j} (\rho v^i) - \left(B^j \frac{\partial \rho}{\partial x^j} \right) \frac{v^i}{\rho} - \frac{B^i}{\rho} \left[\frac{\partial (\rho v^j)}{\partial x^j} - v^j \frac{\partial \rho}{\partial x^j} \right]. \quad (18)$$

The SPH form of this equation is

$$\frac{\mathrm{d}B_a^i}{\mathrm{d}t} = \frac{1}{\rho_a} \sum_b m_b \left(v_{ba}^i B_a^j - B_a^i v_{ba}^j \right) \frac{\partial W_{ab}}{\partial x_a^j}, \quad (19)$$

where v_{ba}^j denotes $(v_b^j - v_a^j)$. Equivalently we can use

$$\frac{\mathrm{d}}{\mathrm{d}t} \left(\frac{B_a^i}{\rho_a} \right) = \frac{1}{\rho_a^2} \sum_b m_b v_{ba}^i B_a^j \frac{\partial W_{ab}}{\partial x_a^j}. \quad (20)$$

As is usual practice in SPH, the density is estimated via a summation over neighbouring particles according to

$$\rho_a = \sum_b m_b W_{ab}, \quad (21)$$

or alternatively using the time derivative of this expression which gives the SPH form of the continuity equation

$$\frac{\mathrm{d}\rho_a}{\mathrm{d}t} = -\sum_b m_b v_{ba}^i \frac{\partial W_{ab}}{\partial x_a^i}. \quad (22)$$

We note that equations (15) and (17) can be derived from a variational principle using (19) and (22) as constraints, demonstrating that these are indeed a consistent set of equations. This is presented in Paper II.

The smoothing kernel we use is the usual spline-based kernel, given by

$$W(q) = \frac{\sigma}{h^\nu} \begin{cases} 1 - \frac{3}{2} q^2 + \frac{3}{4} q^3 & 0 \leqslant q < 1 \\ \frac{1}{4} (2 - q)^3 & 1 \leqslant q < 2 \\ 0 & q \geqslant 2 \end{cases} \quad (23)$$

where $q = |\boldsymbol{r}_a - \boldsymbol{r}_b|/h$, ν is the number of spatial dimensions and the normalization constant σ is given by $2/3$, $10/(7\pi)$ and $1/\pi$ in one, two and three dimensions, respectively. The smoothing length h of particle a is set according to the usual rule

$$h_a \propto \left(\frac{1}{\rho_a} \right)^{(1/\nu)}. \quad (24)$$

We implement this by evolving the smoothing length according to (Benz 1990; Monaghan 1992)

$$\frac{\mathrm{d}h_a}{\mathrm{d}t} = -\frac{h_a}{\nu \rho_a} \frac{\mathrm{d}\rho_a}{\mathrm{d}t}. \quad (25)$$

This works extremely well for the tests presented in this paper since the density is evolved using the continuity equation (22). We note, however, that the dependence of the smoothing length on the density given by (24) can be used to derive (again via a variational principle) a set of discrete equations for both SPH and SPMHD which self-consistently account for the extra terms which arise from this dependence. This set of equations is derived and implemented in Paper II, where we demonstrate that it leads to increased accuracy in the propagation of MHD waves. In particular the formalism derived in Paper II is natural to use when the density is calculated via the

SPH summation (21). In this paper we simply take the average of the kernel to maintain the symmetry in the momentum and energy equations (Hernquist & Katz 1989; Monaghan 1992), that is

$$W_{ab} = \frac{1}{2}\left[W_{ab}(h_a) + W_{ab}(h_b)\right], \tag{26}$$

and correspondingly

$$\frac{\partial W_{ab}}{\partial x_a^i} = \frac{1}{2}\left[\frac{\partial W_{ab}(h_a)}{\partial x_a^i} + \frac{\partial W_{ab}(h_b)}{\partial x_a^i}\right]. \tag{27}$$

4 DISSIPATION TERMS

Chow & Monaghan (1997) discuss the SPH dissipation analogously to that associated with Riemann solvers. The key point is that the dissipation involves jumps in appropriate variables (momentum, energy and density) between the left and right Riemann states multiplied by eigenvalues which can be interpreted as signal velocities. In the SPH case we construct dissipation terms in a similar way. Thus

$$\Pi_{ab} = -\frac{K v_{\rm sig}(\boldsymbol{v}_a - \boldsymbol{v}_b)\cdot \boldsymbol{j}}{\bar{\rho}_{ab}}, \tag{28}$$

where $K \sim 0.5$ is a constant, $v_{\rm sig}$ is a signal velocity, and $\boldsymbol{j}$ is a unit vector from particle b to particle a:

$$\boldsymbol{j} = \frac{\boldsymbol{r}_{ab}}{|\boldsymbol{r}_{ab}|}. \tag{29}$$

The density $\bar{\rho}_{ab} = \frac{1}{2}(\rho_a + \rho_b)$ is an average density. In the relativistic case it was necessary to replace the velocity by the momentum and in the relativistic momentum it was necessary to use the velocity along the line of sight of the two particles in order to guarantee that the viscous dissipation makes a positive contribution to the thermal energy and therefore to the entropy. We will see that similar ideas are required here.

The dissipation in the energy equation can be taken as

$$\Omega_{ab} = -\frac{K v_{\rm sig}(e_a^* - e_b^*)\boldsymbol{j}}{\bar{\rho_{ab}}}, \tag{30}$$

where e^* is an energy quantity which is related to $\widehat{\epsilon}$. Its precise form will now be deduced by considering the rate of change of thermal energy.

From (12) using the SPH equations for the rate of change of velocity, energy, magnetic field and density we find that the magnetic terms cancel leaving

$$\begin{aligned}\frac{{\rm d}u_a}{{\rm d}t} = {} & \frac{P_a}{\rho_a^2}\sum_b m_b v_{ab}^i \frac{\partial W_{ab}}{\partial x_a^i} \\ & + \sum_b m_b \frac{K v_{\rm sig}}{\bar{\rho_{ab}}}\left[(e_a^* - e_b^*)\right. \\ & \left. -(\boldsymbol{v}_a\cdot\boldsymbol{j})(\boldsymbol{v}_a - \boldsymbol{v}_b)\cdot\boldsymbol{j})\right]|\boldsymbol{r}_{ab}|F_{ab},\end{aligned} \tag{31}$$

where $F_{ab}\,\boldsymbol{r}_{ab} = \nabla W_{ab}$, and $F_{ab} \leqslant 0$ is an even function of r_{ab}.

The first term on the right-hand side is the adiabatic change in thermal energy due to the expansion or compression of the gas. This term does not change the entropy. The second term is the contribution to the change in thermal energy due to viscous dissipation, thermal conduction and ohmic heating. Only the first and last of these must contribute a non-negative quantity to the change in the thermal energy. Heat conduction can either increase or decrease the thermal energy of an element of fluid. However, all three must contribute a positive quantity to the change of entropy of the system. The proof that the contribution to the entropy is positive is given in Appendix B. The terms due to viscous dissipation and ohmic dissipation must be negative definite because $F_{ab} \leqslant 0$.

It is natural to try and construct $e*$ using the terms in $\widehat{\epsilon}$, namely

$$\widehat{\epsilon} = \frac{1}{2}v^2 + u + \frac{B^2}{2\mu_0\rho}. \tag{32}$$

4.1 Viscous dissipation

The kinetic energy combined with the velocity terms in (32) is not negative definite and in this form cannot be the correct viscous dissipation. We get a positive definite viscous dissipation in the velocity terms by choosing

$$e_a^* - e_b^* = \frac{1}{2}(\boldsymbol{v}_a\cdot\boldsymbol{j})^2 - \frac{1}{2}(\boldsymbol{v}_b\cdot\boldsymbol{j})^2 + u_a - u_b + \frac{B_a^2}{2\mu_0\rho_a} - \frac{B_b^2}{2\mu_0\rho_b}. \tag{33}$$

We can then write the velocity terms in (31) as

$$-\frac{1}{2}\left[(\boldsymbol{v}_a\cdot\boldsymbol{j}) - (\boldsymbol{v}_b\cdot\boldsymbol{j})\right]^2, \tag{34}$$

which is negative definite. Recalling that $F_{ab} \leqslant 0$ the viscous contribution to the thermal energy is therefore positive. Note that the combination $(e_a^* - e_b^*)$ is not a simple difference because both e_a^* and e_b^* involve $\boldsymbol{j}$ which depends on both particles.

4.2 Ohmic dissipation

The magnetic term is wrong because it can be positive or negative. In addition, it depends on the total field, whereas in a shock we would expect it to involve only the component perpendicular to the shock. We therefore replace the magnetic energy term by using the component of the field perpendicular to the line of sight of the two particles a and b; then we have

$$\begin{aligned}e_a^* - e_b^* = {} & \frac{1}{2}(\boldsymbol{v}_a\cdot\boldsymbol{j})^2 - \frac{1}{2}(\boldsymbol{v}_b\cdot\boldsymbol{j})^2 + u_a - u_b \\ & + \frac{1}{2\mu_0\bar{\rho}_{ab}}\left[B_a^2 - (\boldsymbol{B}_a\cdot\boldsymbol{j})^2 - B_b^2 + (\boldsymbol{B}_b\cdot\boldsymbol{j})^2\right].\end{aligned} \tag{35}$$

The magnetic term is still not negative definite. To make it negative definite we need to add a term

$$\frac{1}{\mu_0\bar{\rho}_{ab}}\left\{(\boldsymbol{B}_a\cdot\boldsymbol{j})\left[(\boldsymbol{B}_a\cdot\boldsymbol{j}) - (\boldsymbol{B}_b\cdot j)\right] - \boldsymbol{B}_a\cdot[\boldsymbol{B}_a - \boldsymbol{B}_b]\right\}. \tag{36}$$

With this new term added the magnetic contribution to the thermal energy becomes

$$-\frac{1}{2\bar{\rho}_{ab}\mu_0}\left[\boldsymbol{B}_{ab}^2 - (\boldsymbol{B}_{ab}\cdot\boldsymbol{j})^2\right], \tag{37}$$

which is negative definite and, when combined with F_{ab}, gives a positive contribution to the thermal energy change.

The interpretation of the extra magnetic terms is quite simple: when currents are present, and the conductivity is finite, the induction equation requires an extra term as in (5). The contribution to the rate of change of thermal energy from the new term is

$$-\frac{\boldsymbol{B}_a}{\mu_0}\cdot\sum_b m_b\frac{K v_{\rm sig}}{\bar{\rho_{ab}}^2}\left[\boldsymbol{B}_{ab} - \boldsymbol{j}(\boldsymbol{B}_{ab}\cdot\boldsymbol{j})\right] r_{ab}F_{ab}. \tag{38}$$

The term which must be added to the induction equation for consistency can be deduced by noting that the expression for the rate of change of thermal energy (12) has a magnetic term

$$-\frac{\rm d}{{\rm d}t}\left(\frac{B^2}{2\rho\mu_0}\right) = -\frac{\boldsymbol{B}}{\rho\mu_0}\frac{{\rm d}\boldsymbol{B}}{{\rm d}t} + \frac{B^2}{\rho^2\mu_0}\frac{{\rm d}\rho}{{\rm d}t}. \tag{39}$$

Comparing the first term with (38) we find that the SPH induction equation requires a term

$$\left.\frac{{\rm d}\boldsymbol{B}_a}{{\rm d}t}\right|_{\rm diss} = \rho_a\sum_b m_b\frac{K v_{\rm sig}}{\bar{\rho}_{ab}^2}[\boldsymbol{j}\times(\boldsymbol{B}_{ab}\times\boldsymbol{j})]r_{ab}F_{ab}, \tag{40}$$

and we expect that the continuum version of this term should be some approximation to

$$-\nabla \times (\eta \nabla \times \boldsymbol{B}), \tag{41}$$

which when η is constant is

$$\eta[\nabla^2 \boldsymbol{B} - \nabla(\nabla \cdot \boldsymbol{B})]. \tag{42}$$

By replacing the summation in (40) by an integral, and expanding in a Taylor series about $\boldsymbol{r}_a$, and assuming that $v_{\rm sig}$ is constant, we find that (40) is proportional to

$$K v_{\rm sig} h \left[\nabla^2 \boldsymbol{B} - \frac{2}{3}\nabla(\nabla \cdot \boldsymbol{B})\right], \tag{43}$$

which is similar to the exact equation with ohmic diffusivity $\eta \propto K v_{\rm sig} h$.

4.3 The signal velocity

We refer the reader to a general discussion of signal velocities in Monaghan (1997) and Chow & Monaghan (1997). The key point is that it is the relative speed of signals from moving observers at the positions of particles a and b when the signals are sent along the line of sight. If there are no magnetic fields a good estimate of this signal velocity is

$$v_{\rm sig} = c_a + c_b - \beta \boldsymbol{v}_{ab} \cdot \boldsymbol{j}, \tag{44}$$

where c_a denotes the speed of sound of particle a and $\beta \sim 1$. The signal velocity is larger when the particles are approaching each other and in practice the effects of shocks can be included by choosing $\beta = 2$ (however, when the artificial dissipation switch discussed in Section 4.4 is used we find it is better to set $\beta = 1$ due to the stronger source term). If there are magnetic fields then a variety of other waves is possible. The fastest wave in a static medium along the x axis has speed

$$\frac{1}{2}\left(\sqrt{c^2 + \frac{B^2}{\rho\mu_0} + \frac{2B^x c}{\sqrt{\rho\mu_0}}} + \sqrt{c^2 + \frac{B^2}{\rho\mu_0} - \frac{2B^x c}{\sqrt{\rho\mu_0}}}\right). \tag{45}$$

A natural generalization of (44) for the case of magnetic fields is to take

$$v_{\rm sig} = v_a + v_b - \beta \boldsymbol{v}_{ab} \cdot \boldsymbol{j}, \tag{46}$$

where

$$v_a = \frac{1}{2}\left(\sqrt{c_a^2 + \frac{B_a^2}{\rho_a\mu_0} + \frac{2\boldsymbol{B}_a \cdot \boldsymbol{j} c_a}{\sqrt{\rho_a\mu_0}}} + \sqrt{c_a^2 + \frac{B_a^2}{\rho_a\mu_0} - \frac{2\boldsymbol{B}_a \cdot \boldsymbol{j} c_a}{\sqrt{\rho_a\mu_0}}}\right), \tag{47}$$

with a similar equation for v_b.

4.4 Artificial dissipation switch

A switch to reduce the artificial viscosity away from shocks is given by Morris & Monaghan (1997). Using this switch together with the suggestions of Balsara (1995) in multi-dimensional simulations can virtually eliminate the problematic effects of using an artificial dissipation in SPH.

The key idea is to regard the dissipation parameter K (cf. equation 28) as a particle property. This can then be evolved along with the fluid equations according to

$$\frac{{\rm d}K_a}{{\rm d}t} = -\frac{K_a - K_{\rm min}}{\tau_a} + \mathcal{S}_a, \tag{48}$$

such that in the absence of sources $\mathcal{S}$, K decays to a value $K_{\rm min}$ over a time-scale τ. The time-scale τ is calculated according to

$$\tau = \frac{h}{\mathcal{C} v_{\rm sig}}, \tag{49}$$

where h is the particle's smoothing length, $v_{\rm sig}$ is the maximum signal propagation speed at the particle location and $\mathcal{C}$ is a dimensionless parameter with value $0.1 < \mathcal{C} < 0.2$. We conservatively use $\mathcal{C} = 0.1$ which means that the value of K decays to $K_{\rm min}$ over about five smoothing lengths.

The source term $\mathcal{S}$ is chosen such that the artificial dissipation grows as the particle approaches a shock front. We use

$$\mathcal{S} = \max(-\nabla \cdot \boldsymbol{v}, 0), \tag{50}$$

such that the dissipation grows in regions of strong compression. Following Morris & Monaghan (1997) where the ratio of specific heats γ differs from 5/3 (but not for the isothermal case), we multiply $\mathcal{S}$ by a factor

$$\left[\ln\left(\frac{5/3+1}{5/3-1}\right)\right] \Big/ \left[\ln\left(\frac{\gamma+1}{\gamma-1}\right)\right]. \tag{51}$$

Note that our source term is a factor of two times larger than the term used by Morris & Monaghan (1997) since our dissipation parameter K is required to be of order $K \sim 0.5$ at a shock front, whilst the usual SPH artificial viscosity parameter α is of order unity. We prefer this stronger source term since it provides sufficient damping in the hydrodynamic shock tube problem of Sod (1978) and in the MHD shock tube tests we describe in this paper (i.e. $K_{\rm max} \sim 0.5$ for these problems).

In order to conserve momentum the average value $\bar{K} = 0.5(K_a + K_b)$ is used in equation (28) or (30). A lower limit of $K_{\rm min} = 0.05$ is used to preserve order away from shocks (note that this is an order of magnitude reduction from the usual value of $K = 0.5$ everywhere).

The numerical tests in Section 7 demonstrate that use of this limiter gives a significant reduction in dissipation away from shocks whilst preserving the shock-capturing ability of the code.

5 INSTABILITY CORRECTION

The tensile instability is corrected via the method proposed by Monaghan (2000). The idea is to add a small term which prevents particles clumping under negative stress. The momentum equation (15) becomes

$$\frac{{\rm d}v_a^i}{{\rm d}t} = \sum_b m_b \left\{\left(\frac{S_{ij}}{\rho^2}\right)_a + \left(\frac{S_{ij}}{\rho^2}\right)_b + R\left[\left(\frac{B_i B_j}{\rho^2}\right)_a + \left(\frac{B_i B_j}{\rho^2}\right)_b\right]\right\} \frac{\partial W_{ab}}{\partial x_{j,a}}, \tag{52}$$

where R is a function which increases as the particle separation decreases, and is given by

$$R = -\frac{\epsilon}{2\mu_0}\left(\frac{W_{ab}}{W(\Delta p)}\right)^n, \tag{53}$$

where W is the SPH kernel and $W(\Delta p)$ is the kernel evaluated at the average particle spacing. Further details of the derivation of this term are given in Appendix A. For all the simulations presented here the particles are set up with $h = 1.5\Delta p$ and therefore in (53) we compute the kernel in the denominator using $\Delta p/h = 1/1.5$. We use $\epsilon = 0.8$ and $n = 5$ throughout this paper and in one dimension we apply the correction only in the x-direction.

Note that where the total energy equation (17) is used, the source term

$$\left.\frac{\mathrm{d}\widehat{\epsilon}_a}{\mathrm{d}t}\right|_{\rm src} = \sum_b m_b v_a^i R\left[\left(\frac{B_i B_j}{\rho^2}\right)_a + \left(\frac{B_i B_j}{\rho^2}\right)_b\right]\frac{\partial W_{ab}}{\partial x_{j,a}}, \qquad (54)$$

is added for consistency.

We show in Section 7 that this correction term very effectively removes the tensile instability with few side-effects.

6 TIME-STEPPING

We integrate the SPMHD equations using a simple mid-point predictor–corrector method. Quantities are predicted according to

$$\boldsymbol{A}^{1/2} = \boldsymbol{A}^0 + \frac{\Delta t}{2}\left(\frac{\mathrm{d}\boldsymbol{A}}{\mathrm{d}t}\right)^{-1/2}, \qquad (55)$$

where

$$\boldsymbol{A} = [x, v_x, v_y, v_z, \rho, \hat{\epsilon}, B_y, B_z, h, K]^{\rm T}, \qquad (56)$$

with the energy $\hat{\epsilon}$ interchangeable for the thermal energy u. Note that we evolve the smoothing length alongside the particle equations as discussed in Section 3 and that the dissipation parameter K is also evolved in accordance with the switch discussed in Section 4.4. The density is also included since in this paper the continuity equation (22) is integrated rather than using the density summation (21).

The rates of change $\mathrm{d}\boldsymbol{A}/\mathrm{d}t$ of these quantities are then computed via the SPH summations using the predicted values $\boldsymbol{A}^{1/2}$. The corrector step is given by

$$\boldsymbol{A}^* = \boldsymbol{A}^0 + \frac{\Delta t}{2}\left(\frac{\mathrm{d}\boldsymbol{A}}{\mathrm{d}t}\right)^{1/2}, \qquad (57)$$

and

$$\boldsymbol{A}^1 = 2\boldsymbol{A}^* - \boldsymbol{A}^0. \qquad (58)$$

The time-step is determined by the Courant condition

$$\mathrm{d}t_c = C_{\rm cour}\min\left(\frac{\bar{h}_{ab}}{v_{{\rm sig},ab}}\right) \qquad (59)$$

where $\bar{h}_{ab} = 0.5(h_a + h_b)$, and the signal velocity $v_{\rm sig}$ is given by equation (46), except that we use

$$v_{{\rm sig},ab} = v_a + v_b + \beta|\boldsymbol{v}_{ab}\cdot\boldsymbol{j}| \qquad (60)$$

with $\beta = 1$ when $\boldsymbol{v}_{ab}\cdot\boldsymbol{j} > 0$ (i.e. where the dissipation terms are not applied). The minimum in (59) is taken over all particle interactions and in this paper we use $C_{\rm cour} = 0.8$.

Although this condition is sufficient for all of the simulations described here, in general it is necessary to pose the additional constraint from the forces

$$\mathrm{d}t_f = \min\left(\frac{h_a}{|\boldsymbol{a}_a|}\right)^{1/2}, \qquad (61)$$

where $\boldsymbol{a}_a$ is the acceleration on particle a.

7 NUMERICAL TESTS IN ONE DIMENSION

The numerical scheme described in this paper has been tested on a variety of one-dimensional problems. In order to demonstrate that SPMHD gives good results on problems involving discontinuities in the physical variables we present results of standard problems used to test grid-based MHD codes (e.g. Stone et al. 1992; Dai & Woodward 1994; Ryu & Jones 1995; Balsara 1998; Dai & Woodward 1998). The advantages of SPMHD are the simplicity with which these results can be obtained and the complete absence of any numerical grid. Further tests (MHD waves) are given in Paper II since they incorporate the use of the variable smoothing length terms.

7.1 Implementation

The particles are allowed to move in one dimension only, whilst the velocity and magnetic field are allowed to vary in three dimensions. We use equal-mass particles such that density changes correspond to changes in particle spacing. Unless otherwise indicated in this paper we integrate the continuity equation (22), the momentum equation (15), the total energy equation (17) and the induction equation (19). This is the most efficient implementation of the SPMHD equations since it does not require an extra pass over the particles to calculate the density via the summation (21). Similar results to those shown here are also obtained when the thermal energy equation is integrated instead of the total energy. Additionally we note that, whilst evolving the flux per unit mass (20) instead of the flux density (19) does not exactly maintain $\nabla\cdot\boldsymbol{B} = 0$ in one dimension, the associated errors are small and hence we also find in this case that the results are similar. Unless otherwise indicated the tests presented here are all performed with the artificial dissipation switch discussed in Section 4.4 turned on with minimum dissipation parameter $K_{\rm min} = 0.05$. This results in very little dissipation away from shock fronts.

7.1.1 Scaling

The magnetic field variable is scaled in units such that the constant μ_0 is unity and numerical quantities are dimensionless. Note that the magnetic flux density $\boldsymbol{B}$ has dimensions

$$[\boldsymbol{B}] = \frac{[\rm mass]}{[\rm time][\rm charge]}, \qquad (62)$$

whilst μ_0 has dimensions

$$[\mu_0] = \frac{[\rm mass][\rm length]}{[\rm charge]^2}. \qquad (63)$$

Choosing mass, length and time-scales of unity and specifying $\mu_0 = 1$ therefore defines the unit of charge. Rescaling of the magnetic field variable to physical units requires multiplication of the code value by a constant

$$\boldsymbol{B}_{\rm physical} = \left\{\frac{\mu_0[\rm mass]}{[\rm length][\rm time]^2}\right\}^{1/2}\boldsymbol{B}_{\rm numerical}. \qquad (64)$$

For example, in cgs units, with mass, length and time-scales of unity the magnetic flux density in gauss is given by

$$\boldsymbol{B}_{\rm cgs} = (4\pi)^{1/2}\boldsymbol{B}_{\rm numerical}. \qquad (65)$$

7.1.2 Initial conditions

Integration of the continuity equation (22) requires some smoothing of the initial conditions and we follow Monaghan (1997) such that when an initial quantity A is discontinuous it is smoothed according to the rule

$$A = \frac{A_{\rm L} + A_{\rm R}\mathrm{e}^{x/d}}{1 + \mathrm{e}^{x/d}} \qquad (66)$$

where $A_{\rm L}$ and $A_{\rm R}$ are the uniform left and right states with respect to the origin and d is taken as half of the largest initial particle separation at the interface (i.e. the particle separation on the low-density

side). Note, however, that we *do not* smooth the initial velocity profiles except in the rarefaction test. Where the initial density is smoothed the particles are spaced according to the rule

$$\rho_a(x_{a+1} - x_{a-1}) = 2\rho_{\rm R}\Delta_{\rm R} \tag{67}$$

where $\Delta_{\rm R}$ is the particle spacing to the far right of the origin with density $\rho_{\rm R}$. Note that initial smoothing lengths are set according to the rule $h \propto 1/\rho$ and are therefore also smoothed. Where the total energy $\hat{\epsilon}$ is integrated we smooth the basic variables u and $\boldsymbol{B}$ and construct the total energy from (10). There is some inconsistency in the smoothing in this case as it is not possible self-consistently to construct smooth profiles of ρ, u, B_y, B_z and $\hat{\epsilon}$ with the above smoothing. This can cause a small glitch in the initial conditions when the total energy equation is used.

Such smoothing of the initial conditions can be avoided altogether if the density summation (21) is used, particularly if the smoothing length is updated self-consistently with the density. This is demonstrated in Paper II.

7.1.3 Boundaries

Boundary conditions are implemented in one dimension by simply fixing the properties of the six particles closest to each boundary. Where the initial velocities of these particles are non-zero their positions are evolved accordingly and a particle is removed from the domain once it has crossed the boundary. Where the distance between the closest particle and the boundary is more than the initial particle spacing a new particle is introduced to the domain. Hence for inflow or outflow boundary conditions the resolution changes throughout the simulation.

7.1.4 Dissipative terms

Direct application of the dissipation terms described in Section 4 provides no smoothing for the velocity in the y- (and z-) directions since we use $(\boldsymbol{v}_a - \boldsymbol{v}_b) \cdot \boldsymbol{j}$ in equation (28) and the particles are restricted to move along the x-axis only. If the particles were allowed to move in the $y(z)$-direction (with velocity $v_z(v_z)$) such smoothing would naturally be present. Therefore in the simulations presented in this paper we use

$$\Pi_{ab} = -\frac{K v_{\rm sig}(\boldsymbol{v}_a - \boldsymbol{v}_b) \cdot \hat{\boldsymbol{v}}}{\bar{\rho}_{ab}}, \tag{68}$$

where $\hat{\mathbf{v}}$ is a unit vector along the direction of the particle velocities given by

$$\hat{\boldsymbol{v}} = \frac{\boldsymbol{v}_a - \boldsymbol{v}_b}{|\boldsymbol{v}_a - \boldsymbol{v}_b|}. \tag{69}$$

The term in the momentum equation is then

$$\sum_b m_b \Pi_{ab} \hat{\boldsymbol{v}} G_{ab}, \tag{70}$$

where we note that the gradient of the kernel may be written as $\nabla_a W_{ab} = \boldsymbol{j} G_{ab}$, which we replace with $\hat{\boldsymbol{v}} G_{ab}$ where G_{ab} is a scalar function (note that $G_{ab} = F_{ab} h/|\boldsymbol{r}_{ab}|$).

In the dissipative energy we use

$$e_a^* = \frac{1}{2}(v_a \cdot \hat{\boldsymbol{v}})^2 + u_a + \frac{1}{2}(\boldsymbol{B}_a \cdot \boldsymbol{j})^2, \tag{71}$$

with the contribution to the thermal energy equation from the kinetic terms given by

$$-\frac{1}{2}\left[(\boldsymbol{v}_a \cdot \hat{\boldsymbol{v}}) - (\boldsymbol{v}_b \cdot \hat{\boldsymbol{v}})\right]^2. \tag{72}$$

Note that the dissipative terms are only applied where $\boldsymbol{v}_{ab} \cdot \boldsymbol{j} > 0$.

7.2 Simple advection test

This simple test is described in Evans & Hawley (1988) and in Stone et al. (1992) and measures the ability of an algorithm to advect contact discontinuities. A square pulse of transverse magnetic field is set up and advected a distance of five times its width with the pressure terms switched off. The current density $\boldsymbol{J}$ is calculated in order to ascertain that the method does not produce sign reversals or anomalous extrema in this quantity. In SPH we compute this quantity using

$$\boldsymbol{J}_a = \nabla \times \boldsymbol{B}_a = \sum_b m_b(\boldsymbol{B}_a - \boldsymbol{B}_b) \times \nabla_a W_{ab}. \tag{73}$$

We perform this test simply by using a magnetic pressure that is negligible compared to the gas pressure. We set up 100 particles placed evenly along the x-axis with constant velocity in the positive x-direction and use a pulse that is initially 50 particle spacings wide. The pulse is not initially smoothed in any way and periodic boundary conditions are enforced using ghost particles (this is also a good test of the periodic boundary conditions since the particles are continually crossing the domain).

The SPMHD results are shown in Fig. 1 after advecting the pulse a distance of five times its width (in this case five crossings of the computational domain). The top panel shows the results with the artificial dissipation terms turned off. The spread in the discontinuities is kept to less than a particle spacing, showing no visible dispersion or diffusion whatsoever, suggesting that SPH indeed handles contact discontinuities very well. The current density, which is analytically given by a delta function at each discontinuity, is also computed very well by the SPH approximation (see Monaghan 1992). When the dissipative terms are turned on using the switch (Section 4.4) a small smoothing of the field is observed (bottom panels); however this still compares favourably with the schemes shown in Stone et al. (1992).

7.3 Shock tubes

The first shock tube test we perform was first described by Brio & Wu (1988) and is the MHD analogue of the shock tube problem of Sod (1978). The problem consists of a discontinuity in pressure, density, transverse magnetic field and internal energy initially located at the origin. As time develops, complex shock structures develop which only occur in MHD because of the different wave types. Specifically the problem of Brio & Wu (1988) contains a compound wave consisting of a slow shock attached to a rarefaction wave. The existence of such intermediate shocks was contrary to the expectations of earlier theoretical studies (Brio & Wu 1988). This problem is now a standard test for any astrophysical MHD code and has been used by many authors (e.g. Stone et al. 1992; Dai & Woodward 1994; Ryu & Jones 1995; Balsara 1998).

We set up the problem using approximately 800 equal-mass particles in the domain $x = [-0.5, 0.5]$. Initial conditions to the left of the discontinuity (hereafter the left state) are given by $(\rho, P, v_x, v_z, B_y) = [1, 1, 0, 0, 1]$ and conditions to the right (hereafter the right state) are given by $(\rho, P, v_x, v_z, B_y) = [0.125, 0.1, 0, 0, -1]$ with $B_x = 0.75$ and $\gamma = 2.0$. The results are shown in Fig. 2 at time $t = 0.1$ and compare well with the numerical solution in Balsara (1998) (solid lines). Similar results to Fig. 2 are obtained when the thermal energy equation is integrated.

In the second shock tube test (Fig. 3), we demonstrate the usefulness of the artificial dissipation switch by considering a problem which involves both a fast and slow shock. We consider the

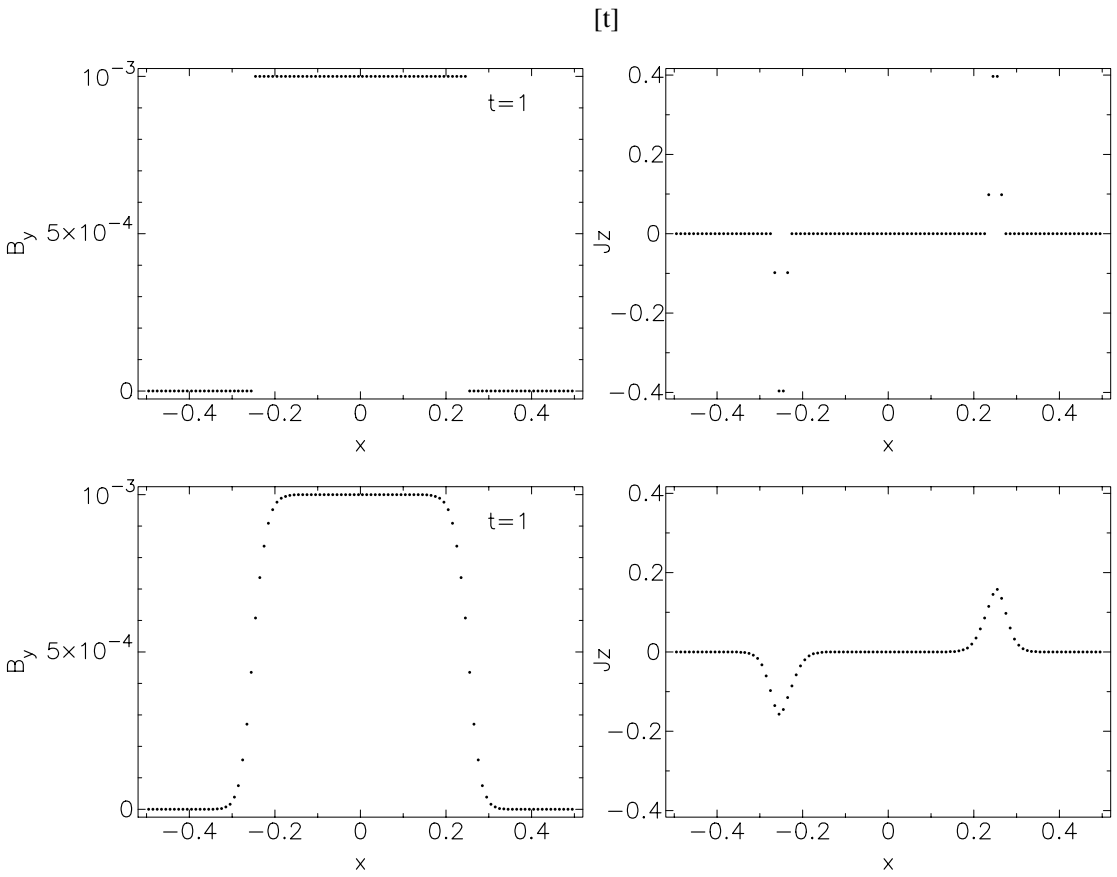

Figure 1. Results of the advection of a square pulse of transverse magnetic field 50 particle separations wide over a distance of five times its width. In the absence of dissipative terms the discontinuities are kept to less than a particle spacing (top) and the current density (top right) shows almost no spread (analytically this is a delta function at each discontinuity). With the dissipative terms included with the switch of Morris & Monaghan (1997) a small amount of smoothing is observed (bottom panels).

Riemann problem with left state $(\rho, P, v_x, v_z, B_y) = [1, 1, 0, 0, 1]$ and the right state $(\rho, P, v_x, v_z, B_y) = [0.2, 0.1, 0, 0, 0]$ with $B_x = 1$ and $\gamma = 5/3$. This test has been used by Dai & Woodward (1994), Ryu & Jones (1995) and Balsara (1998) and illustrates the formation of a switch-on fast shock. Similarly to the previous test we set up the simulation using approximately 800 particles in the domain $x = [-0.5, 0.5]$. The results are shown in Fig. 3 at time $t = 0.15$ and compare well with the exact solution given by Ryu & Jones (1995) (solid lines). The advantages of the dissipation switch are apparent in this problem since it contains both a fast and slow shock. In a run with dissipation parameter $K = 0.5$ everywhere the fast shock is significantly damped. In Fig. 3 we see that the fast shock is resolved, although some small oscillations are observed behind the shock front. These oscillations can be removed entirely by using a slightly higher minimum dissipation parameter ($K_{\rm min} = 0.1$).

The third test illustrates the formation of seven discontinuities in the same problem (Fig. 4). The left state is given by $(\rho, P, v_x, v_z, v_z, B_y, B_z) = [1.08, 0.95, 1.2, 0.01, 0.5, 3.6/(4\pi)^{1/2}, 2/(4\pi)^{1/2}]$ and the right state by $(\rho, P, v_x, v_z, v_z, B_y, B_z) = [1, 1, 0, 0, 0, 4/(4\pi)^{1/2}, 2/(4\pi)^{1/2}]$ with $B_x = 2/(4\pi)^{1/2}$ and $\gamma = 5/3$. Since the velocity in the x-direction is non-zero at the boundary, we continually inject particles into the left half of the domain with the appropriate left state properties. The resolution therefore varies from an initial 700 particles to 875 particles at $t = 0.2$. The results are shown in Fig. 4 at time $t = 0.2$. The SPMHD solution compares extremely well with the exact solution taken from Ryu & Jones (1995) (solid line) and may also be compared with the numerical solution in that paper and in Balsara (1998). The thermal energy and density profiles are slightly improved by our use of the total energy equation. Note that the initial velocity profiles are not smoothed for this problem, resulting in the small starting error at the contact discontinuity.

The fourth test (Fig. 5) is similar to the previous version except that an isothermal equation of state is used. The left state is given by $(\rho, v_x, v_z, v_z, B_y, B_z) = [1.08, 1.2, 0.01, 0.5, 3.6/(4\pi)^{1/2}, 2/(4\pi)^{1/2}]$ and the right state by $(\rho, v_x, v_z, v_z, B_y, B_z) = [1, 0, 0, 0, 4/(4\pi)^{1/2}, 2/(4\pi)^{1/2}]$ with $B_x = 2/(4\pi)^{1/2}$ and an isothermal sound speed of unity. Results are shown in Fig. 5 at time $t = 0.2$ and compare very well with the numerical results given in Balsara (1998) (solid line).

The fifth test shows the formation of two magnetosonic rarefactions. The left state is given by $(\rho, P, v_x, v_z, B_y) = [1, 1, -1, 0, 1]$ and the right state by $(\rho, P, v_x, v_z, B_y) = [1, 1, 1, 0, 1]$ with $B_x = 0$ and $\gamma = 5/3$. Results are shown in Fig. 6 at time $t = 0.1$ and compare extremely well with the exact solution from Ryu & Jones (1995) (solid line). Outflow boundary conditions are used such that the resolution varies from an initial 500 particles down to 402 particles at $t = 0.1$ in the domain $x = [-0.5, 0.5]$. The artificial dissipation switch is turned on with $K_{\rm min} = 0.05$ although very little dissipation occurs in this simulation since the artificial dissipation is only applied for particles approaching each other. With unsmoothed initial conditions we therefore observe some oscillations behind the

[t]

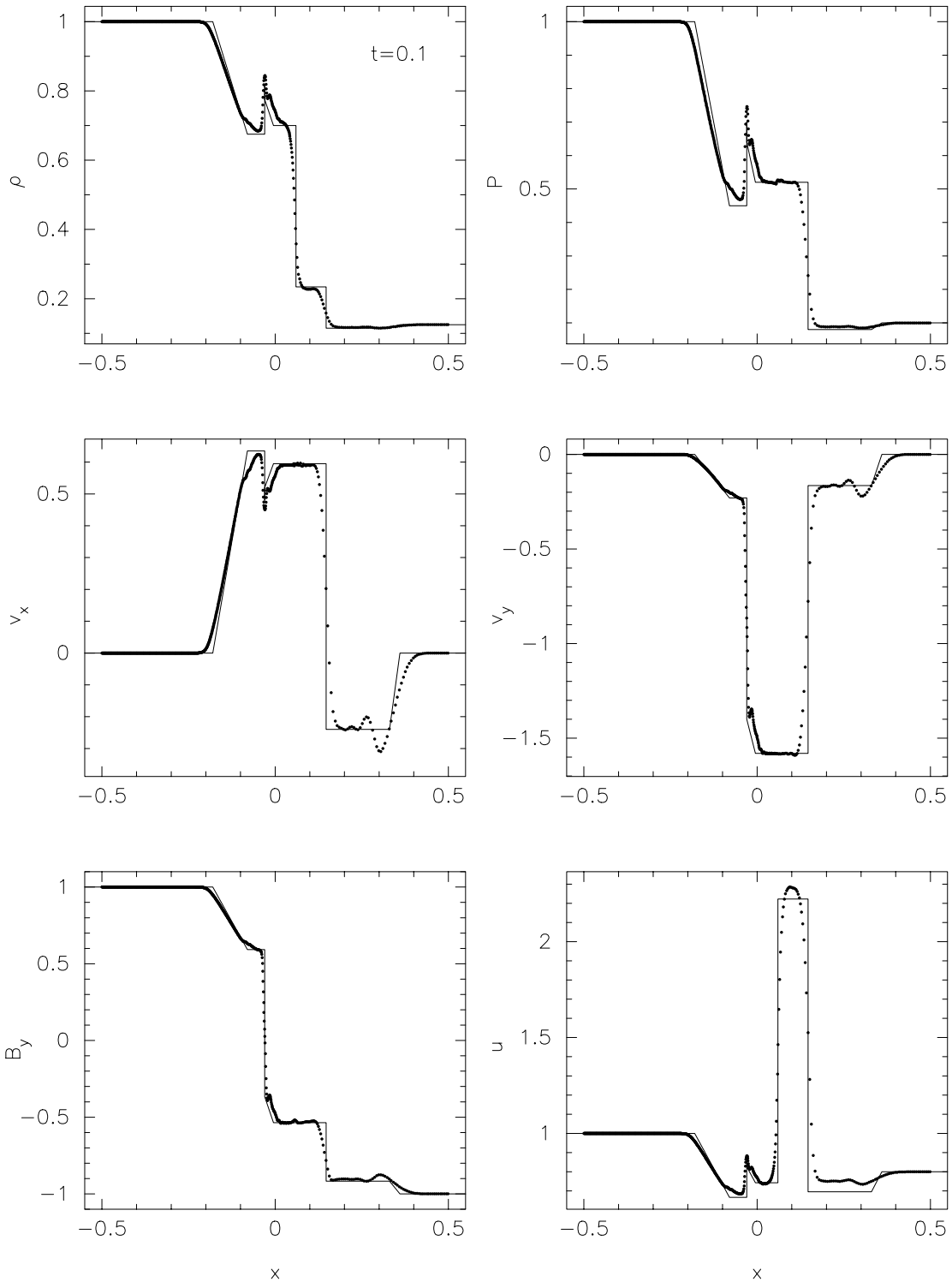

Figure 2. Results of the shock tube test of Brio & Wu (1988). To the left of the origin the initial state is $(\rho, P, v_x, v_z, B_y) = [1, 1, 0, 0, 1]$ whilst to the right the initial state is $(\rho, P, v_x, v_z, B_y) = [0.125, 0.1, 0, 0, -1]$ with $B_x = 0.75$ everywhere and $\gamma = 2.0$. Profiles of density, pressure, v_x, v_z, thermal energy and B_y are shown at time $t = 0.1$. Points indicate the SPMHD particles whilst the numerical solution from Balsara (1998) is given by the solid line. The artificial dissipation switch with $K_{\rm min} = 0.05$ is used.

[t]

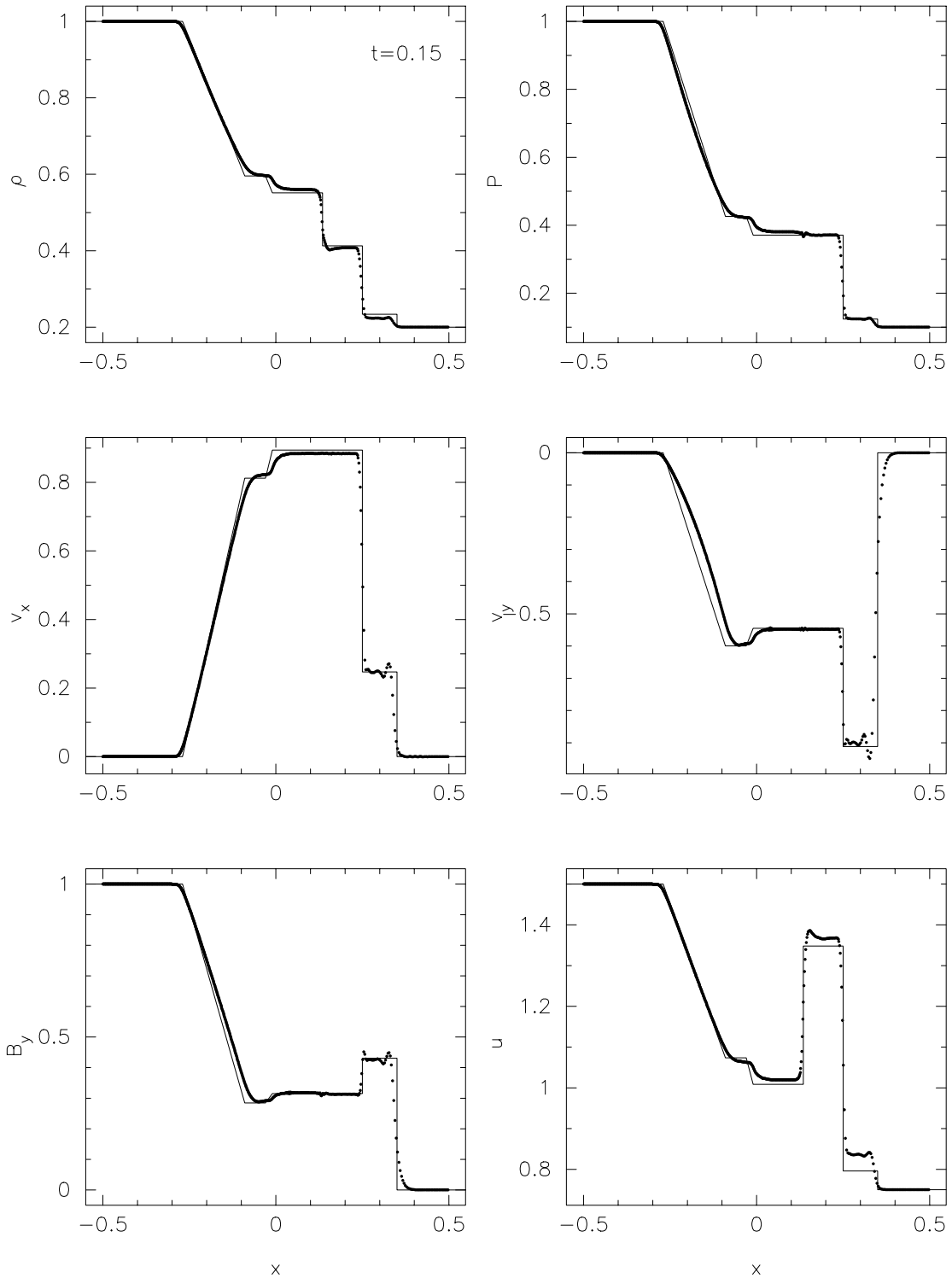

Figure 3. Results of the MHD shock tube test with left state $(\rho, P, v_x, v_z, B_y) = [1, 1, 0, 0, 1]$ and right state $(\rho, P, v_x, v_z, B_y) = [0.2, 0.1, 0, 0, 0]$ with $B_x = 1$ and $\gamma = 5/3$ at time $t = 0.15$. The problem illustrates the formation of a switch-on fast shock and the solution contains both a fast and slow shock. Solid points indicate the SPMHD particles whilst the exact solution is given by the solid line. The artificial dissipation switch is used. Without this switch the fast shock is significantly damped.

[t]

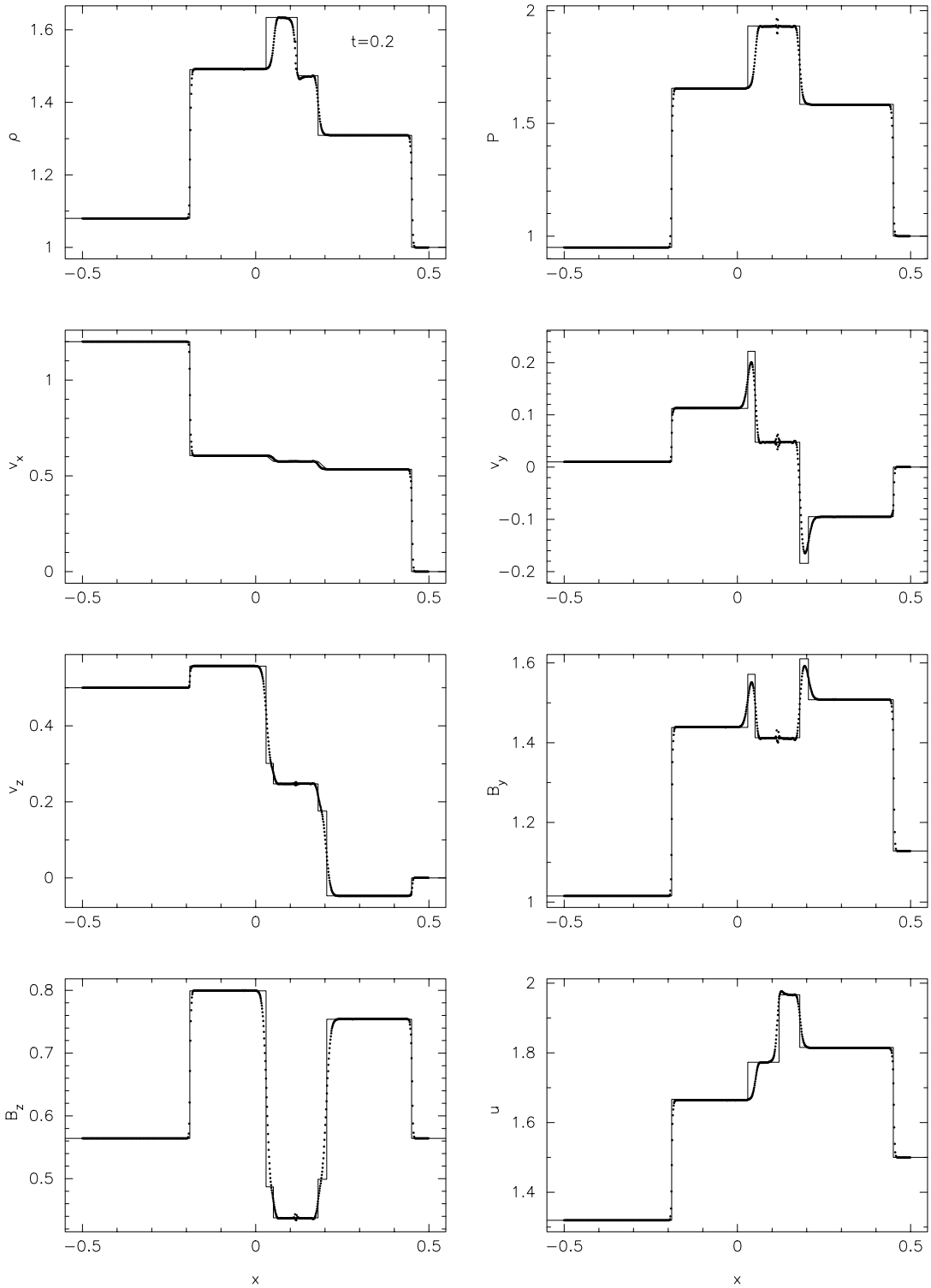

Figure 4. Results of the MHD shock tube test with left state $(\rho, P, v_x, v_z, v_z, B_y, B_z) = [1.08, 0.95, 1.2, 0.01, 0.5, 3.6/(4\pi)^{1/2}, 2/(4\pi)^{1/2}]$ and right state $(\rho, P, v_x, v_z, v_z, B_y, B_z) = [1, 1, 0, 0, 0, 4/(4\pi)^{1/2}, 2/(4\pi)^{1/2}]$ with $B_x = 2/(4\pi)^{1/2}$ and $\gamma = 5/3$ at time $t = 0.2$. This problem illustrates the formation of seven discontinuities. The exact solution is given by the solid line whilst points indicate the positions of the SPMHD particles. The artificial dissipation switch is used with $K_{\rm min} = 0.05$.

[t]

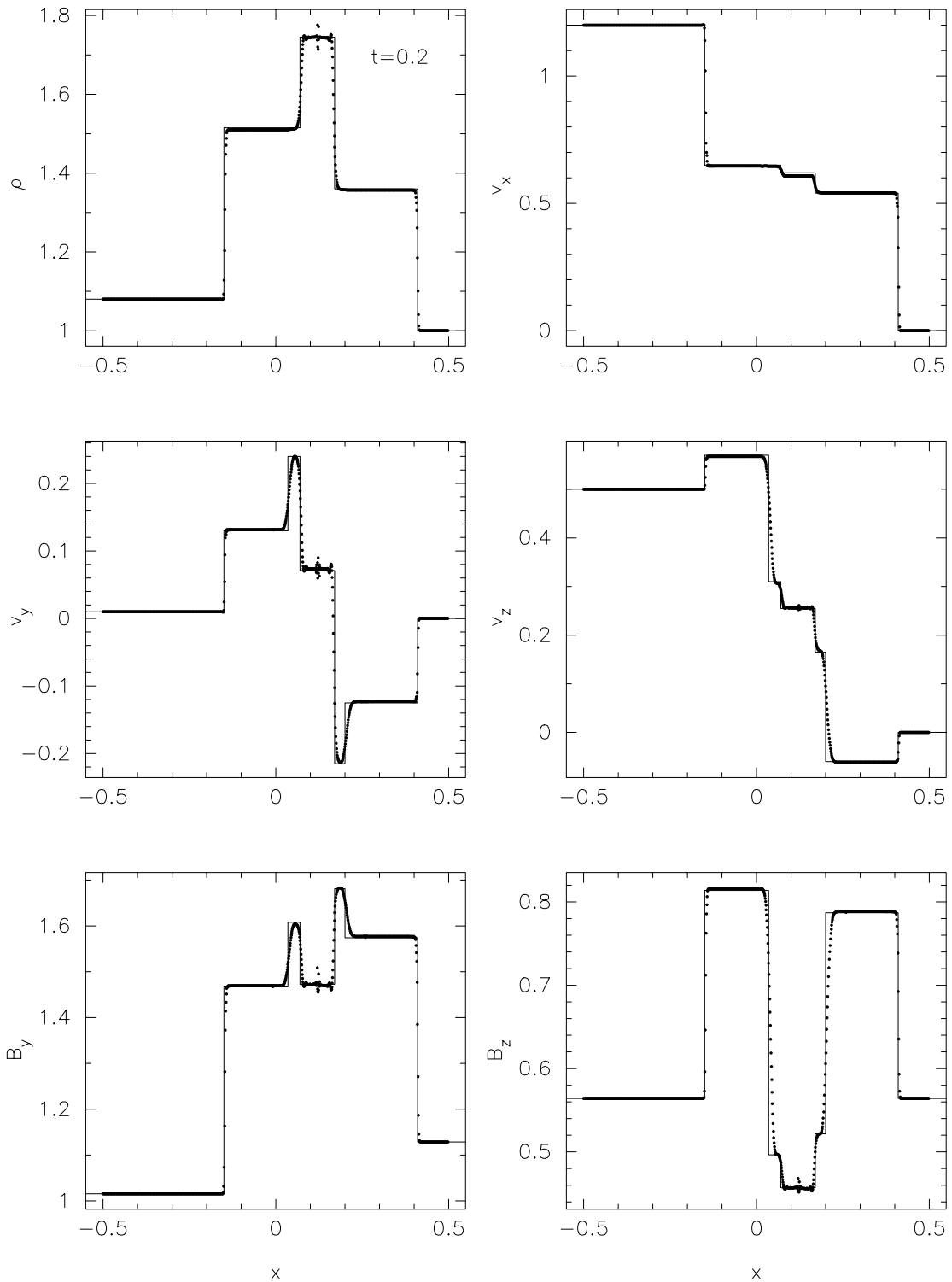

Figure 5. Results of the isothermal MHD shock tube test with left state $(\rho, v_x, v_z, v_z, B_y, B_z) = [1.08, 1.2, 0.01, 0.5, 3.6/(4\pi)^{1/2}, 2/(4\pi)^{1/2}]$ and right state $(\rho, P, v_x, v_z, v_z, B_y, B_z) = [1, 0, 0, 0, 4/(4\pi)^{1/2}, 2/(4\pi)^{1/2}]$ with $B_x = 2/(4\pi)^{1/2}$ and an isothermal sound speed of unity at time $t = 0.2$. This problem illustrates the formation of six discontinuities in isothermal MHD. Solid points indicate the position of the SPMHD particles which may be compared with the exact solution given by the solid line. The artificial dissipation switch is used with $K_{\rm min} = 0.05$.

[t]

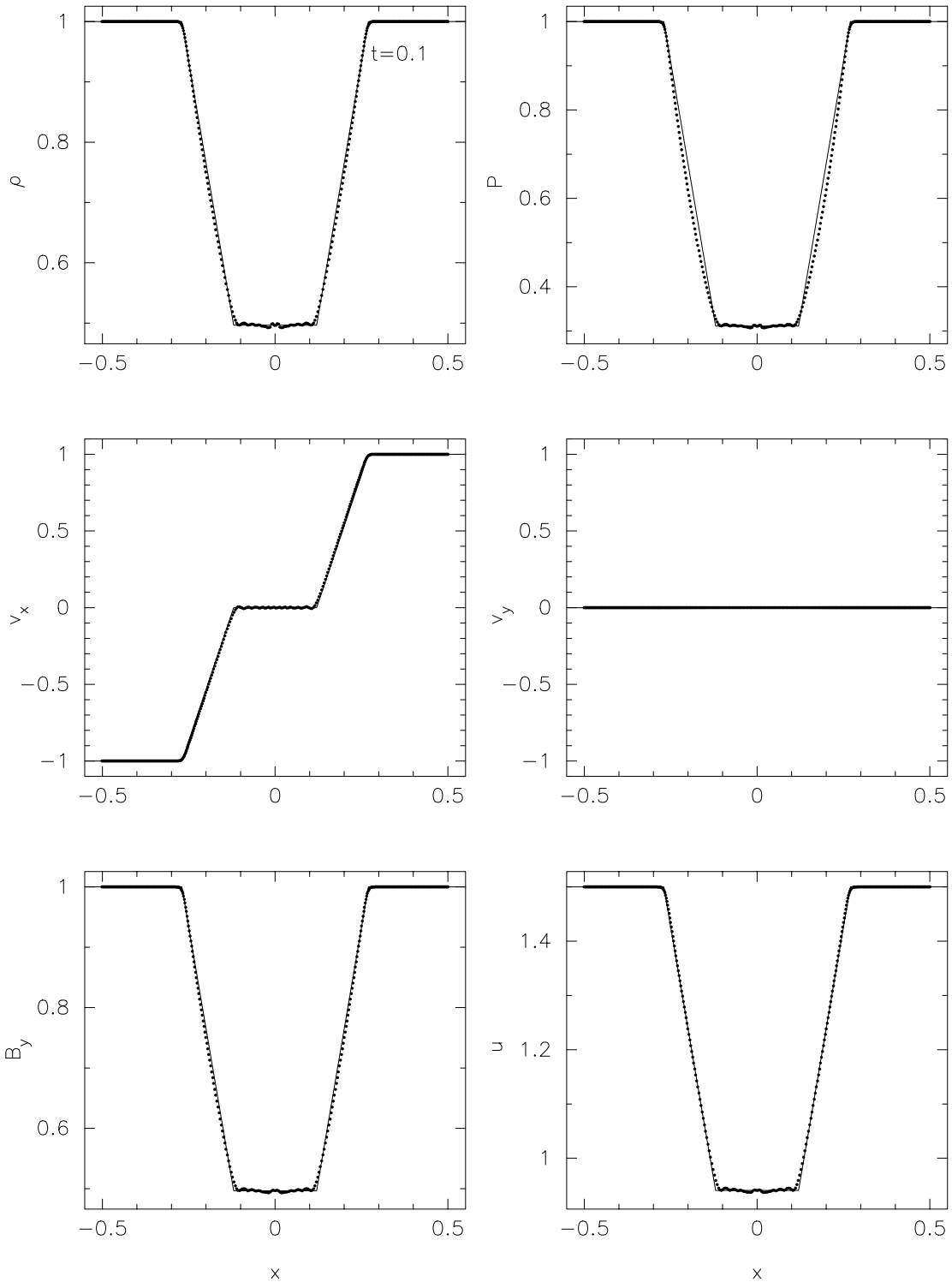

Figure 6. Results of the MHD shock tube test with left state $(\rho, P, v_x, v_z, B_y) = [1, 1, -1, 0, 1]$ and right state $(\rho, P, v_x, v_z, B_y) = [1, 1, 1, 0, 1]$ with $B_x = 0$ and $\gamma = 5/3$ at time $t = 0.1$. This problem illustrates the formation of two magnetosonic rarefactions. The exact solution is given by the solid line whilst points indicate the position of the SPMHD particles. The artificial dissipation switch is used with $K_{\rm min} = 0.05$.

rarefaction waves, which are removed in this case by smoothing the initial discontinuity slightly. As noted in Monaghan (1997) use of the density summation also improves the results for this type of problem.

The final test, taken from Dai & Woodward (1994) and Balsara (1998), illustrates the formation of two fast shocks, each with Mach number 25.5. The left state is given by $(\rho, P, v_x, v_z, v_z, B_y, B_z) = [1, 1, 36.87, -0.155, -0.0386, 4/(4\pi)^{1/2}, 1/(4\pi)^{1/2}]$ and the right

[t]

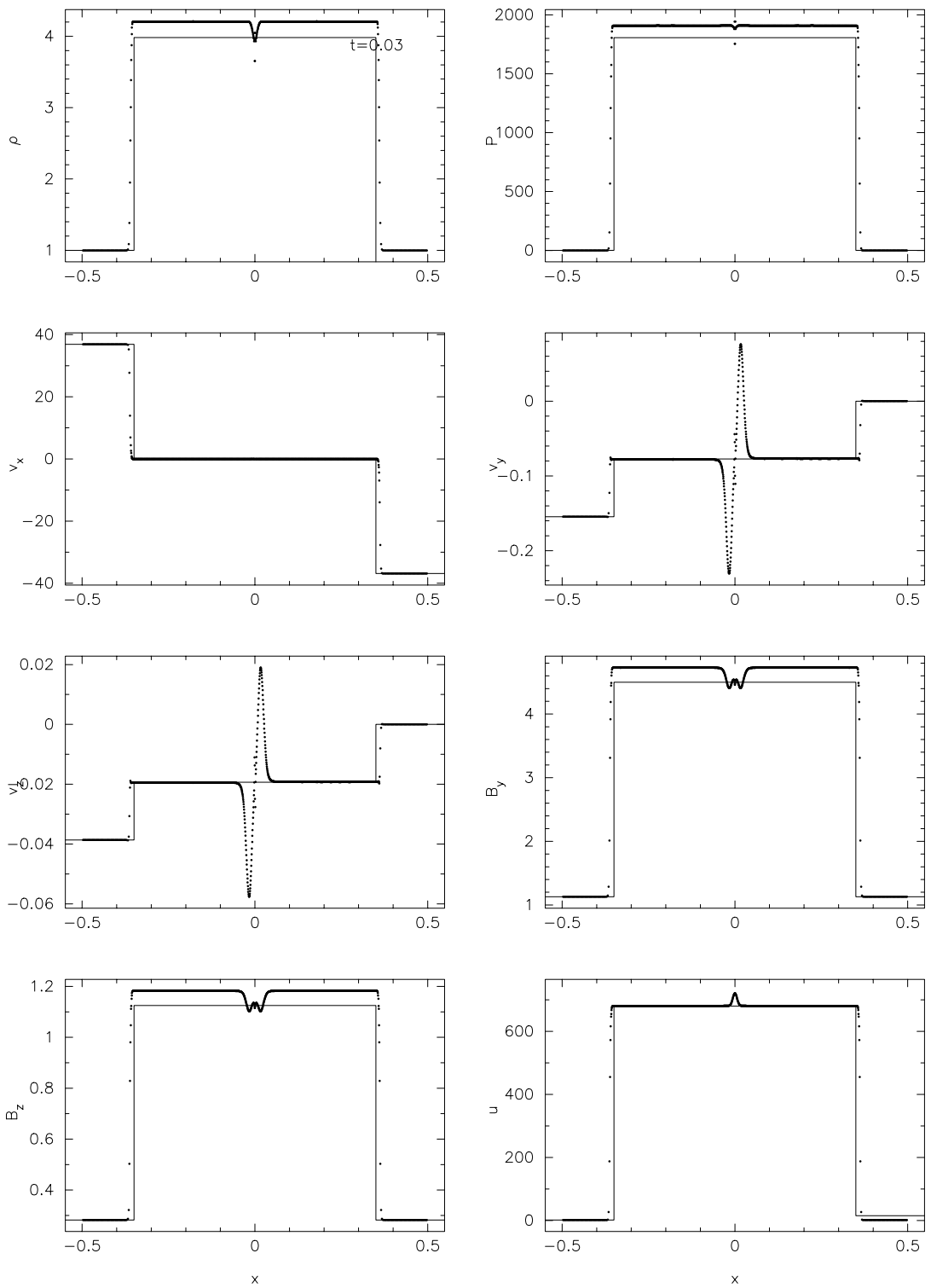

Figure 7. Results of the MHD shock tube test with left state $(\rho, P, v_x, v_z, v_z, B_y, B_z) = [1, 1, 36.87, -0.155, -0.0386, 4/(4\pi)^{1/2}, 1/(4\pi)^{1/2}]$ and right state $(\rho, P, v_x, v_z, v_z, B_y, B_z) = [1, 1, -36.87, 0, 0, 4/(4\pi)^{1/2}, 1/(4\pi)^{1/2}]$ with $B_x = 4.0/(4\pi)^{1/2}$ and $\gamma = 5/3$. Results are shown at time $t = 0.03$. This problem illustrates the formation of two extremely strong fast shocks of Mach number 25.5 each. Solid points indicate the position of the SPH particles whilst the exact solution is given by the solid line. The artificial dissipation switch is used with $K_{\rm min} = 0.05$. The overshoots in density, pressure and magnetic field are a result of our integration of the continuity equation and neglect of terms relating to the gradient of the smoothing length (these terms are derived in Paper II).

state by $(\rho, P, v_x, v_z, v_z, B_y, B_z) = [1, 1, -36.87, 0, 0, 4/(4\pi)^{1/2}, 1/(4\pi)^{1/2}]$ with $B_x = 4.0/(4\pi)^{1/2}$ and $\gamma = 5/3$. Results are shown in Fig. 7 at time $t = 0.03$. Inflow boundary conditions are used such that the resolution varies from an initial 400 particles up to 1286 particles at $t = 0.03$ in the domain $x = [-0.5, 0.5]$. The artificial dissipation switch is turned on with $K_{\min} = 0.05$. The results compare extremely well with the exact solution (solid line) given by Dai & Woodward (1994) and with the numerical solution given by Dai & Woodward (1994) and Balsara (1998), especially given the extreme nature of the problem. The spikes in transverse velocity components are starting errors due to the fact that for this problem we do not smooth the initially discontinuous velocity profiles in any way. There is some advantage to integrating the total energy equation for this type of problem since using the thermal energy equation produces a large spike in thermal energy at the discontinuity and numerical noise behind the shocks. The overshoots in density, pressure and magnetic field are a result of our integration of the continuity equation and neglect of terms relating to the gradient of the smoothing length. These terms are derived and implemented in Paper II and can be shown to remove the errors seen here.

8 SUMMARY

We have shown how SPH equations for MHD can be formulated with the following features:

(i) The equations use the continuum equations of Janhunen (2000) and Dellar (2001) which are consistent even when the divergence of the magnetic field is non-zero. Consequently, even though non-zero $\nabla \cdot \boldsymbol{B}$ may be produced during the simulation, it is treated consistently. We find that insisting on consistency with fundamental principles is the key to deriving stable SPH equations.

(ii) The equations contain artificial dissipation. We require these dissipation terms to result in positive definite changes to the entropy and this places strong constraints on the form of the dissipation. Our equations guarantee that the resulting viscous and ohmic dissipation produces positive changes in the thermal energy. In ensuring these equations are consistent with the fundamental requirement that the entropy should increase we are led to introduce a term in the induction equation which is analogous to the induction equation for non-ideal MHD. The use of the switch of Morris & Monaghan (1997) very effectively minimizes the effect of the artificial dissipation away from shocks.

(iii) The SPMHD equations also incorporate a simple technique to prevent an instability due to the tension arising from the magnetic stress.

The resulting equations, when implemented with a simple predictor–corrector scheme, give good results for a wide range of shock tube problems. While we have yet to apply our algorithm to problems in two and three dimensions the present results encourage us to believe that our SPMHD code will provide a secure basis for astrophysical MHD problems.

ACKNOWLEDGMENTS

DJP acknowledges the support of the Association of Commonwealth Universities and the Cambridge Commonwealth Trust. He is supported by a Commonwealth Scholarship and Fellowship Plan. DJP would also like to acknowledge useful discussions with Prof J. E. Pringle.

REFERENCES

Balsara D. S., 1995, J. Comp. Phys., 121, 357
Balsara D. S., 1998, ApJS, 116, 133
Benz W., 1984, A&A, 139, 378
Benz W., 1990, in Buchler J. R., ed., The numerical modelling of nonlinear stellar pulsations. Kluwer, Dordrecht, p. 269
Bonet J., Kulasegaram S., 2000, Int. J. Numer. Meth. Eng., 47, 1189
Bonet J., Kulasegaram S., 2001, Int. J. Numer. Meth. Eng., 52, 1203
Børve S., 2001, PhD thesis, Univ. Oslo
Børve S., Omang M., Trulsen J., 2001, ApJ, 561, 82
Brackbill J. U., Barnes D. C., 1980, J. Comp. Phys., 35, 426
Brio M., Wu C. C., 1988, J. Comp. Phys., 75, 400
Byleveld S. E., Pongracic H., 1996, Publ. Astron. Soc. Aust., 13, 71
Cerqueira A. H., de Gouveia Dal Pino, 2001, ApJ, 560, 779
Chow E., Monaghan J. J., 1997, J. Comp. Phys., 134, 296
Cleary P. W., Monaghan J. J., 1999, J. Comp. Phys., 148, 227
Dai W., Woodward P. R., 1994, J. Comp. Phys., 115, 485
Dai W., Woodward P. R., 1998, ApJ, 494, 317
Dellar P. J., 2001, J. Comp. Phys., 172, 392
Dolag K., Bartelmann M., Lesch H., 1999, A&A, 348, 351
Dyka C. T., Randles P. W., Ingel R. P., 1997, Int. J. Numer. Meth. Eng., 40, 2325
Evans C. R., Hawley J. F., 1988, ApJ, 332, 659
Gingold R. A., Monaghan J. J., 1977, MNRAS, 181, 375
Gray J., Monaghan J. J., Swift R. P., 2002, Comput. Meth. Appl. Mech. Eng, 190, 6641
Habe A., Uchida Y., Ikeuchi S., Pudritz R. E., 1991, PASJ, 43, 703
Harten A., Lax P. D., Van Leer B., 1983, SIAM Rev., 25, 35
Hernquist L., Katz N., 1989, ApJS, 70, 419
Hosking J. G., 2002, PhD thesis, Cardiff Univ.
Janhunen P., 2000, J. Comp. Phys., 160, 649
Mac Low M., Klessen R., Burkert A., Smith M., 1999, in Franco J., Carraminana A., eds, Interstellar Turbulence Decay Timescales of MHD Turbulence in Molecular Clouds. Cambridge Univ. Press, Cambridge, p. 256
Marinho E. P., Andreazza C. M., Lépine J. R. D., 2001, A&A, 379, 1123
Meglicki Z., 1994, Comput. Phys. Commun., 81, 91
Meglicki Z., 1995, PhD thesis, Australian National Univ., Canberra
Meglicki Z., Wickramasinghe D., Dewar R. L., 1995, MNRAS, 272, 717
Monaghan J. J., 1992, Ann. Rev. Astron. Astrophys., 30, 543
Monaghan J. J., 1997, J. Comp. Phys., 136, 298
Monaghan J. J., 2000, J. Comp. Phys., 159, 290
Morris J. P., 1996, PhD thesis, Monash Univ., Melbourne
Morris J. P., Monaghan J. J., 1997, J. Comp. Phys., 136, 41
Murray J., Wadsley J., Bond J. R., 1996, BAAS, 28, 1413
Phillips G. J., 1982, Proc. Astron. Soc. Aust., 4, 371
Phillips G. J., 1983a, Proc. Astron. Soc. Aust., 5, 180
Phillips G. J., 1983b, PhD thesis, Monash Univ., Melbourne
Phillips G. J., 1985, Proc. Astron. Soc. Aust., 6, 205
Phillips G. J., 1986a, MNRAS, 221, 571
Phillips G. J., 1986b, MNRAS, 222, 111
Phillips G. J., Monaghan J. J., 1985, MNRAS, 216, 883
Powell K. G., 1994, An approximate Riemann solver for magnetohydrodynamics (that works in more than one dimension). ICASE report 94-24, NASA Langley Research Center (http://techreports.larc.nasa.gov/ltrs/dublincore/1994/icase-1994-24.html)
Powell K. G., Roe P. L., Linde T. J., Gombosi T. I., de Zeeuw D. L., 1999, J. Comp. Phys., 154, 284
Price D. J., Monaghan J. J., 2003, MNRAS, accepted (Paper II)
Ryu D., Jones T. W., 1995, ApJ, 442, 228
Sod G. A., 1978, J. Comp. Phys., 27, 1
Stellingwerf R. F., Peterkin R. E., 1990, Smooth particle magnetohydrodynamics. Technical Report MRC/ABQ-R-1248, Mission Research Corp., Albuquerque, NM
Stellingwerf R. F., Peterkin R. E., 1994, Mem. Soc. Astron. Ital., 65, 991
Stone J. M., Norman M. L., 1992, ApJS, 80, 791

Stone J. M., Hawley J. F., Evans C. R., Norman M. L., 1992, ApJ, 388, 415
Tóth G., 2000, J. Comp. Phys., 161, 605

APPENDIX A: ARTIFICIAL STRESS

In this Appendix we describe some of the details of the artificial stress required to prevent clumping. We diagonalize the magnetic part of the stress tensor by rotating the coordinate system so that the z-axis lies along the magnetic field. The magnetic field is then $\boldsymbol{B}' = (0, 0, B)$ and the stress tensor has non-zero components $M'_{xx} = -B^2/(2\mu_0)$, $M'_{yy} = -B^2/(2\,\mu_0)$ and $M'_{zz} = B^2/(2\mu_0)$. The sign of the first two is associated with compression and the sign of the third is associated with tension. To remove the tension term at close range we add a term to M'_{zz} so that it is negative when the particles approach. The term we choose is RB^2, where

$$R = -\frac{\epsilon}{2\mu_0}\left[\frac{W_{ab}}{W(\Delta p)}\right]^n \tag{A1}$$

where $\epsilon \sim 0.4$ and $n \sim 4$ and in the tests shown in this paper we have $\epsilon = 0.8$ and $n = 5$. The precise values of these quantities is not important. W_{ab} is the kernel and $W(\Delta p)$ is W evaluated at the average particle spacing.

Rotating back to the original coordinates we find that the term we subtracted is equivalent to defining a new magnetic stress

$$M'_{ij} = M_{ij} + RB_iB_j. \tag{A2}$$

APPENDIX B: POSITIVITY OF THE ENTROPY CHANGE

In this Appendix we demonstrate that the dissipation terms introduced in Section 4 lead to a positive definite increase in the entropy.

The second law of thermodynamics shows that the change of entropy per unit mass s_a of particle a is given by

$$T_a\frac{\mathrm{d}s_a}{\mathrm{d}t} = \frac{\mathrm{d}u_a}{\mathrm{d}t} - \frac{P_a}{\rho_a^2}\frac{\mathrm{d}\rho_a}{\mathrm{d}t}, \tag{B1}$$

where T_a is the (absolute) temperature of particle a.

From (31), (34) and (37), and noting that the second term of (B1), when expressed in SPH form, cancels the first term of (31), we find that

$$T_a\frac{\mathrm{d}s_a}{\mathrm{d}t} = \sum_b \frac{m_bKv_{\rm sig}}{\bar{\rho_{ab}}}\left(-[\boldsymbol{v}_a\cdot\boldsymbol{j} - \boldsymbol{v}_b\cdot\boldsymbol{j}]^2 - \frac{1}{\mu_0\bar{\rho}_{ab}}\left[\boldsymbol{B}_{ab}^2 - (\boldsymbol{B}_{ab}\cdot\boldsymbol{j})^2\right] + u_a - u_b\right)r_{ab}F_{ab}. \tag{B2}$$

Because $F_{ab} \leqslant 0$ we can rewrite this equation as

$$T_a\frac{\mathrm{d}s_a}{\mathrm{d}t} = Q_a + \sum_b \frac{m_bKv_{\rm sig}}{\bar{\rho}_{ab}}(u_a - u_b)r_{ab}F_{ab}, \tag{B3}$$

where $Q_a \geqslant 0$ is the contribution to the entropy change from the viscous and ohmic dissipation which we have shown is positive definite. The second term is a heat conduction term which can increase or decrease the thermal energy of a particle but it must not result in a decrease of the entropy of the system. Note that if $u_a > u_b$ then the thermal conduction causes a decrease in the thermal energy of particle a. This form of the conduction term that arises here is similar to that derived by Cleary & Monaghan (1999) for SPH heat conduction problems.

The change in the total entropy S is then

$$\frac{\mathrm{d}S}{\mathrm{d}t} = \sum_a m_a\frac{\mathrm{d}s_a}{\mathrm{d}t} = \sum_a\frac{m_aQ_a}{T_a} + \sum_a\sum_b \zeta_{ab}\frac{(u_a - u_b)}{T_a}, \tag{B4}$$

where

$$\zeta_{ab} = \frac{m_bKv_{\rm sig}r_{ab}F_{ab}}{\bar{\rho}_{ab}} \leqslant 0. \tag{B5}$$

We can interchange the labels in the second term of (B4) and combine with the original form to write this term as

$$\frac{1}{2}\sum_a\sum_b \zeta_{ab}(u_a - u_b)\left(\frac{1}{T_a} - \frac{1}{T_b}\right). \tag{B6}$$

If, as is normally the case, u is a monotonically increasing function of T then, if $T_a > T_b$ we have $u_a > u_b$ and

$$(u_a - u_b)\left(\frac{1}{T_a} - \frac{1}{T_b}\right) \leqslant 0 \tag{B7}$$

so that the second term on the right-hand side of (B4) is positive. The change in the entropy due to thermal conduction is therefore positive.

This paper has been typeset from a TEX/LATEX file prepared by the author.